

Electron cyclotron resonance plasma enhanced direct current sputtering discharge with magnetic-mirror plasma confinement

M. Mišina,^{a)} Y. Setsuhara, and S. Miyake

Joining and Welding Research Institute, Osaka University, 11-1 Mihogaoka, Ibaraki, Osaka 567, Japan

(Received 25 October 1996; accepted 24 January 1997)

Plasma confinement in a mirror magnetic field was applied to the electron cyclotron resonance (ECR) plasma enhanced dc sputtering discharge sustained at pressures below 10^{-2} Pa. Ion current densities up to 12 mA/cm^2 , plasma densities about 10^{11} cm^{-3} and electron temperatures about 25 eV were measured by a Langmuir probe. The cathode current was maximum when the ECR zone was close to the cathode $z_{\text{ECR}} < 10 \text{ cm}$ (measured from the center of the cathode). A mirror ratio $MR \geq 3$ was necessary for sustaining the discharge at simultaneously large microwave powers and cathode voltages. An application of the system studied to the ion assisted deposition of metallic and compound thin films with a controlled crystal structure is proposed. © 1997 American Vacuum Society. [S0734-2101(97)02004-6]

I. INTRODUCTION

Microwave electron cyclotron resonance (ECR) plasma enhanced sputtering (hereafter abbreviated as ECR sputtering) is an advanced deposition technique developed during the last decade.¹⁻⁷ Ionization and excitation of the working medium by a microwave ECR discharge result in low working pressures down to 5×10^{-3} Pa, large substrate ion fluxes of $1-10 \text{ mA/cm}^2$ and in a high reactivity of the molecular gas. A number of examples of the beneficial influence of the microwave ECR plasma enhancement of the sputtering discharge on the deposition of various types of thin films can be found in the literature.⁸⁻¹⁵

One of the advantages of ECR sputtering is the low working pressure. A good confinement of plasma electrons along magnetic field lines is crucial for the operation of the ECR discharge at pressures of about 10^{-2} Pa and lower. In principle, the electrons can be reflected back into the plasma by a negative potential of an electrode (electrostatic confinement) or by the force $F_{e\parallel} = -\mu_e \text{grad}_{\parallel} B$ (magnetic confinement), where $\mu_e = \frac{1}{2} m_e v_{e\perp}^2 / B$ is the magnetic moment of an electron with the velocity $v_{e\perp}$, m_e is the electron mass and $\text{grad}_{\parallel} B$ is the gradient of the magnetic flux density B . The symbols \parallel and \perp denote vector components parallel and perpendicular to the magnetic field.

The configuration of the ECR sputtering which includes a divergent magnetic field and a hollow cylindrical cathode¹⁻³ employs a combination of electrostatic and magnetic confinements (EMCs) of electrons along magnetic field lines. A confinement between two electrostatic mirrors is employed in the system with a planar cathode and a cylindrical cathode connected by magnetic field lines.⁶ This is in principle similar to the magnetron, where a number of magnetic field lines crosses the same cathode. ECR sputtering with a magnetron was also studied.^{5,7,16,17} A pure magnetic field confinement in the mirror field has not yet been tested

for ECR sputtering. Such a system could provide a steady operation at very low pressures $p < 10^{-2}$ Pa with a large ion flux to a substrate. The microwave ECR discharge in the mirror magnetic field has been used previously in the plasma fusion research and for the ion sources. However, it is not clear to what extent the presence of the cathode and of the sputtered metal atoms will affect the discharge characteristics.

The present article is devoted to the investigation of ECR sputtering with plasma confinement in a mirror magnetic field and a hollow cylindrical cathode located in the plane of symmetry of the magnetic trap. The measurements of the cathode current and plasma parameters as a function of the discharge parameters (cathode voltage U_d , microwave power P_{μ} , argon pressure p , spatial distribution of the magnetic field) are reported.

II. EXPERIMENTAL DETAILS

A schematic of the microwave ECR sputtering apparatus with the magnetic-mirror plasma confinement is presented in Fig. 1. A water-cooled stainless steel vacuum chamber of 135 mm in inner diameter (i.d.) was equipped with a cylindrical water-cooled hollow cathode with a copper target. The target was 100 mm in length and 110 mm in i.d. The part of the chamber between the flange (with a waveguide) and the cathode was approximately 200 mm in length.

The magnetic field was produced by two identical coils. The spatial distribution of the magnetic field was modified by the variation of the distance of coils v and/or by the use of a yoke. The yoke consisted of two 8 mm thick soft iron plates that were placed at the "inner" side of the coils, see Fig. 1. The main characteristics of the magnetic field distribution are the mirror ratio (MR), i.e., the ratio of the magnetic field at the throat and at the bottom of the magnetic trap and the axial distance of the ECR zone from the center of the cathode z_{ECR} ; see Fig. 1. Both MR and z_{ECR} are increased by increasing coil distance v or by using the yoke. A larger mirror ratio is achieved for the same z_{ECR} when the yoke is used.

^{a)}Permanent address: Institute of Physics, Academy of Sciences of the Czech Republic, Na Slovance 2, 180 40 Praha 8, Czech Republic; Electronic mail: misina@fzu.cz

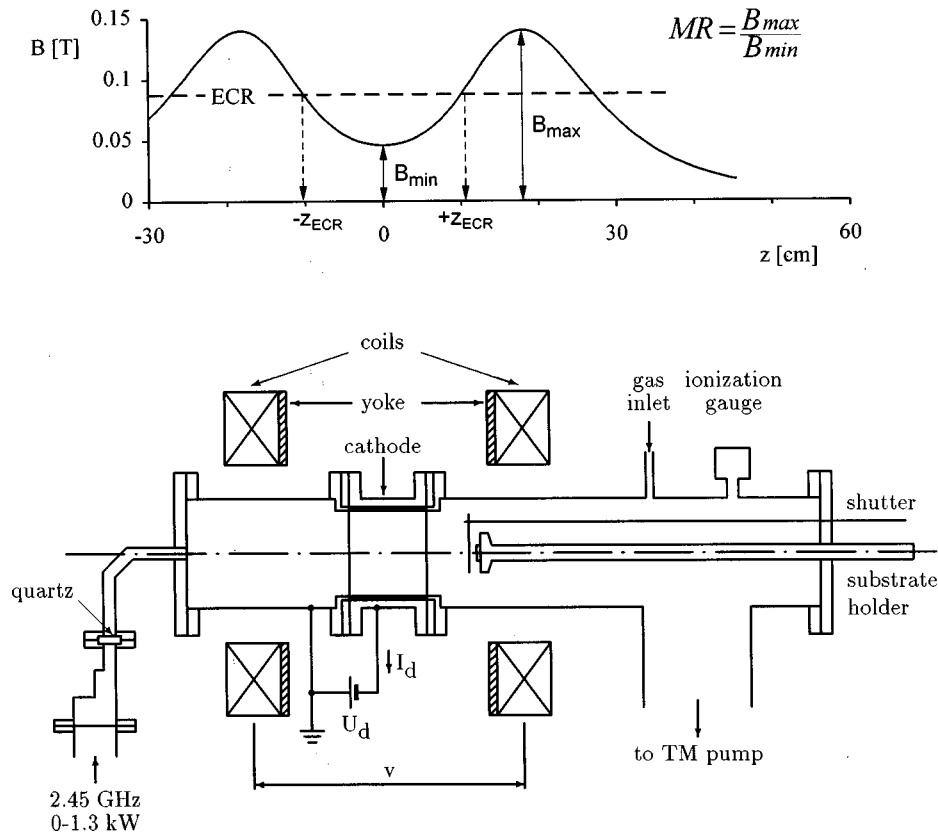


FIG. 1. Schematic of the ECR plasma enhanced dc sputtering apparatus with magnetic-mirror plasma confinement. An axial distribution of the magnetic flux density B at the axis is shown in the upper part for coil current $I_c = 420$ A and coil distance $v = 35$ cm.

Microwaves of 2.45 GHz frequency and up to 1.3 kW power were launched into the plasma along the apparatus axis by direct coupling of a rectangular waveguide with the vacuum chamber. The microwave transmission line consisted of a magnetron, a ferrite isolator with a dummy load, an E-H tuner and a quarter-wavelength transformer to a narrow waveguide followed by an E corner that coupled the waveguide to the vacuum chamber. A quartz window between the transformer and the E corner was used to seal the vacuum. An E corner of the 104 mm \times 54.6 mm cross section was used in first experiments. In this case the quartz window was screened from atoms sputtered from the cathode; however it was covered by the material from the inner wall of the waveguide sputtered by the plasma ions accelerated in the gradient of the magnetic field and in the plasma sheath. No deposits were observed on the quartz window after many hours of operation after replacing the E corner with a narrow 104 mm \times 13.1 mm cross-sectional one with a double bend. The incident microwave power was inferred from the anode current of the magnetron while the reflected power was measured by a crystal sensor attached to a directional coupler in the side branch of the ferrite isolator.

The vacuum chamber was evacuated by a turbomolecular pump (500 ℓ/s) to the base pressure $p_0 \leq 1.5 \times 10^{-4}$ Pa. The discharge was operated in argon at pressures ranging from 4×10^{-3} Pa to 2×10^{-1} Pa. The pressure was adjusted by the

argon flow. The values given in this article refer to the readings of the ionization gauge prior to the ignition of the discharge. The actual pressures in the discharge region could differ considerably from these values due to gas heating, enhanced desorption and burnout of the gas in the plasma.^{18,19} As we had no control over the gas pressure in the region of discharge, only these nominal values are given.

An axially and radially movable planar Langmuir probe was used for measurements of plasma parameters (plasma and floating potentials, plasma density, electron temperature). The probe consisted of the tip of a molybdenum wire 2 mm in diameter, shielded by a ceramics tube. The probe was constructed in such a way that measurements could be made during deposition of the metal films. An electrically floating metal plate with a slot for the Langmuir probe was used for the radial distribution measurements of the plasma parameters. The metal plate stabilized the plasma which was only slightly affected by the probe position as confirmed by a minor variation of the reflected microwave power and of the cathode current with the radial position of the probe.

III. RESULTS AND DISCUSSION

A. Discharge characteristics

Operation of the ECR sputtering discharge was possible in the pressure range from 4×10^{-3} Pa to 2×10^{-2} Pa. The

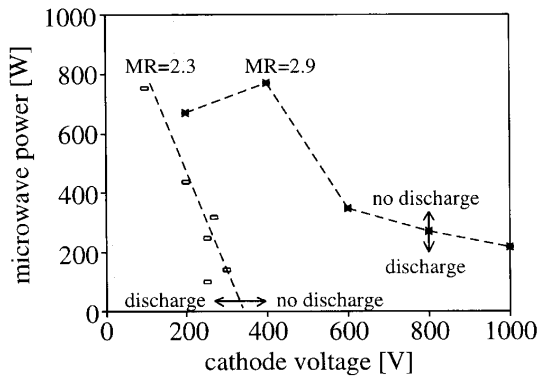


FIG. 2. The microwave power-cathode voltage parameter space of the self-sustained discharge for $p = 5 \times 10^{-3}$ Pa and two mirror ratios, $MR = 2.3$ and $MR = 2.9$. The substrate holder was not in the vacuum chamber.

ECR discharge was generally not self-sustained at lower pressures, although under some conditions we obtained discharge even for $p < 4 \times 10^{-3}$ Pa. However, in these cases a faint light emission from the plasma seemed to originate from a narrow channel around the device axis and only small cathode currents of about 10 mA were measured. This is not enough for an efficient sputter deposition and therefore we did not pay more attention to this plasma mode. A microwave breakdown occurred inside the vacuum part of the waveguide at pressures higher than 2×10^{-2} Pa. Most of microwave energy was then absorbed before entering the discharge chamber and, consequently, the cathode current was again too small.

In the test without the substrate holder in the vacuum chamber it was found that the discharge is not self-sustained when large microwave powers and large cathode voltages are used simultaneously. This is quite opposite to the case of EMC, where at pressures lower than 10^{-2} Pa the discharge is self-sustained only when a sufficiently high negative bias is applied to the cathode.²⁰ In the present case, the border of the

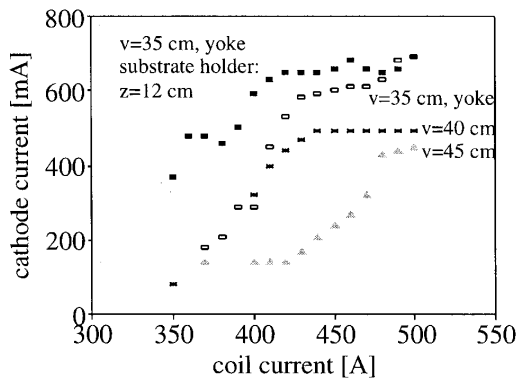


FIG. 3. Cathode current as a function of the coil current for $p = 5 \times 10^{-3}$ Pa, $U_d = 300$ V, $P_\mu = 200$ W and various configurations of magnetic coils. From the uppermost curve: coil distance $v = 35$ cm, yoke, substrate holder (SH) at $z_s = 12$ cm; $v = 35$ cm, yoke, without SH; $v = 40$ cm, without SH; $v = 45$ cm, without SH.

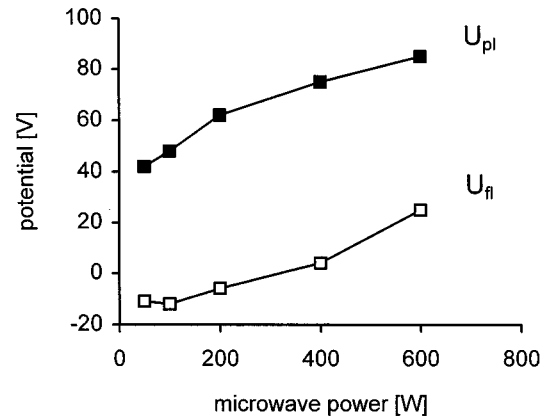
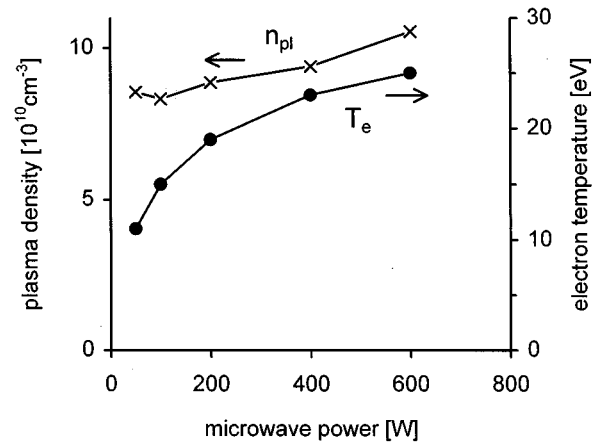


FIG. 4. Plasma density, electron temperature, plasma and floating potentials as a function of microwave power measured at $z = 8$ cm and $r = 0$ cm for $U_d = 0$ V, $p = 5 \times 10^{-3}$ Pa, $z_{\text{ECR}} = 10$ cm and $MR = 2.9$.

region of the self-sustained discharge in the microwave power-cathode voltage parameter space moves to higher values with increasing mirror ratio MR ; see Fig. 2. The values of P_μ and U_d which are available for $MR = 2.9$ already enable sputtering with a reasonable deposition rate. Moreover, the discharge became self-sustained up to $P_\mu = 1.3$ kW and $U_d = 1$ kV (maximum outputs of the sources used in the experiment) when an electrically floating substrate holder was placed close to the ECR zone, further distant from the microwave launcher, see Fig. 1. The cathode current also was increased in this case; see Fig. 3. On the other hand, the discharge was extinguished by a positive bias (about +25 V) of the substrate holder.

All these phenomena can be explained by changes in the confinement of plasma electrons:

- (1) With increasing microwave power the electron temperature increases; see Fig. 4. Larger electron temperature results in larger diffusion coefficients of electrons (e.g., $D_B = kT_e/16B$ for the Bohm diffusion across the magnetic field), i.e. the losses of electrons increase.
- (2) The electrons are confined in the plasma also thanks to the potential well, i.e. by the large positive plasma potential U_{pl} . $U_{pl} \approx 60$ V was measured by the Langmuir

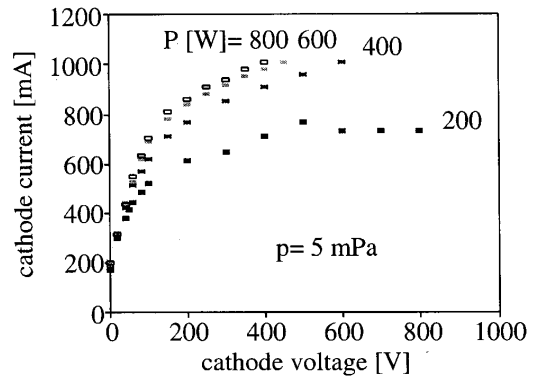
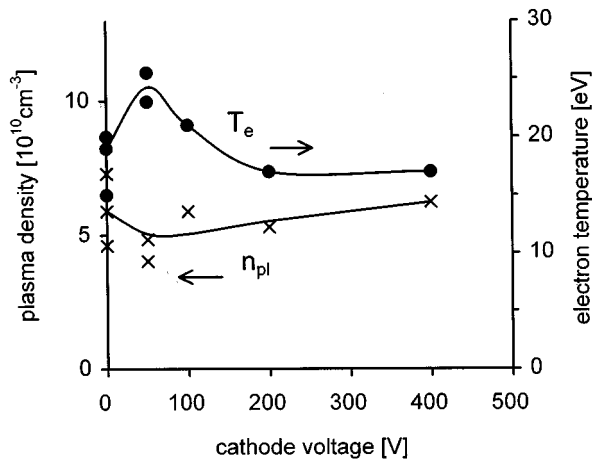


FIG. 7. I - V characteristics of the ECR sputtering discharge for $p=5 \times 10^{-3}$ Pa, various P_μ , $z_{\text{ECR}}=10$ cm, $MR=2.9$ and $z_s=12$ cm.

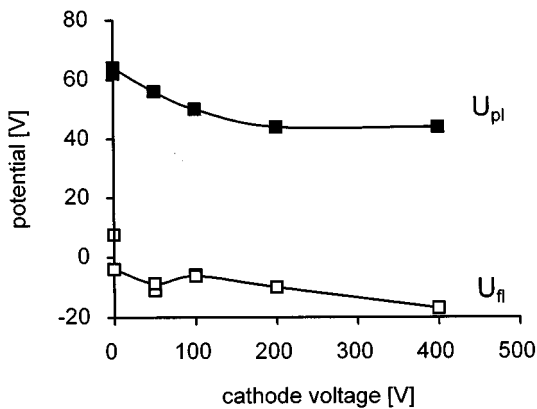


FIG. 5. Plasma density, electron temperature, plasma and floating potentials as a function of cathode voltage measured at $z=9$ cm and $r=0$ cm for $P_\mu=200$ W, $p=5 \times 10^{-3}$ Pa, $z_{\text{ECR}}=10$ cm and $MR=2.9$.

probe. This positive plasma potential decreases with increasing negative bias of the cathode to $U_{pl} \approx 40$ V (see Fig. 5) and the electron losses increase again.

- (3) In the mirror machine of the present geometry the electrons escape from the plasma mainly along the chamber axis, i.e., along magnetic field lines. Confinement is im-

proved by increasing the mirror ratio or by inserting an electrically floating plate which reflects all the electrons with the parallel component of energy smaller than $e(U_{pl} - U_{fl})$, where e is the electron charge and U_{fl} is the floating potential.

The efficiency of the method for sputter deposition was characterized by measurement of the cathode current I_d as a function of process parameters: magnetic coil current I_c , cathode voltage U_d , pressure p and microwave power P_μ .

I_d increases with increasing I_c until $I_c = I_{cr}$ and then saturates; see Fig. 3. I_{cr} is a function of the magnetic field distribution. We compared various parameters of the magnetic field distributions for $I_c = I_{cr}$: the magnetic flux densities at the bottom and at the throat of the trap, the gradient of the magnetic field at the ECR position and the distance z_{ECR} of the ECR zone from the center of the cathode. Among those parameters it was the distance z_{ECR} that exhibited the smallest scattering being 10–11 cm in three cases and 7 cm in one case.²¹ We conclude that small $z_{\text{ECR}} < 10$ cm is the most relevant condition for achieving the maximum cathode current.

I_d as a function of P_μ or U_d can be described in a similar way; see Figs. 6 and 7: first a rapid increase with P_μ (U_d)

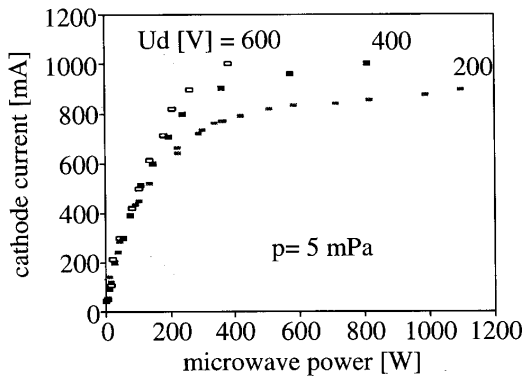


FIG. 6. Cathode current as a function of the microwave power for $p=5 \times 10^{-3}$ Pa, various U_d , $z_{\text{ECR}}=10$ cm, $MR=2.9$ and $z_s=12$ cm.

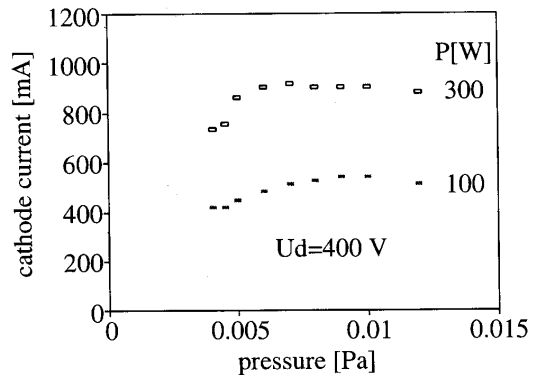


FIG. 8. Cathode current as a function of the argon pressure for $U_d=400$ V, $P_\mu=100$ W and 300 W, $z_{\text{ECR}}=10$ cm, $MR=2.9$, $z_s=12$ cm.

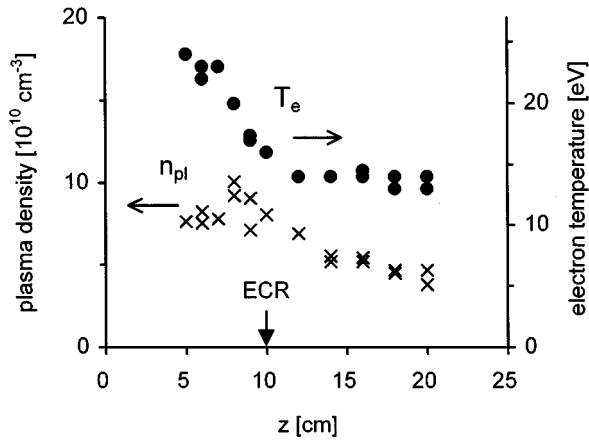


FIG. 9. Plasma density and electron temperature as a function of axial position z for $U_d=0$ V, $P_\mu=200$ W, $p=5\times 10^{-3}$ Pa, $z_{\text{ECR}}=10$ cm and $MR=2.9$.

increasing up to 300 W (200 V), then a much smaller increase or even saturation. I_d varied only slightly with the pressure; see Fig. 8.

B. Langmuir probe measurement of plasma parameters

Floating and plasma potentials U_{fl} and U_{pl} , electron temperature T_e and plasma density n_{pl} were measured by means of a plane Langmuir probe (LP) for 5×10^{-3} Pa pressure and for the magnetic field configuration which was characterized by $z_{\text{ECR}}=10$ cm and $MR=2.9$. Plasma density was inferred from the saturated ion current density i_{sat}^+ and T_e using the equation $n_{pl}=i_{sat}^+(m_i/kT_e)^{1/2}/e$, where k is the Boltzmann constant and m_i is the ion mass.

The axial distributions of T_e and n_{pl} confirm that the plasma is confined between the ECR zones as was reported by Arata *et al.*;²² see Fig. 9. The absolute values of $n_{pl}\approx 10^{11}$ cm $^{-3}$ and $T_e\approx 15$ –20 eV are smaller and larger, respectively, than the values reported by Junck and Getty¹⁸ for the magnetic-mirror confined plasma and the same pressure and microwave power as in the present experiment.

The comparison of the radial distributions of n_{pl} , T_e , U_{fl} and U_{pl} for $U_d=0$ V and 600 V at the axial position $z=12$ cm is presented in Fig. 10. The negative bias of the cylindrical cathode results in (i) reduction of U_{pl} from about +60 V to +30 V; (ii) decrease of T_e , which is especially large at large diameters $r\geq 3$ cm, where the electrons are probably cooled down by collisions with sputtered atoms; (iii) homogeneous distribution of n_{pl} for radii $r\leq 3$ cm; and (iv) a sharp, large peak of n_{pl} at $r=3.5$ cm with its value at the maximum twice as large as n_{pl} for $r\leq 3$ cm. The location of this peak at $r=3.5$ cm and $z=12$ cm is connected along a magnetic field line with the cathode surface, whose position is given by $r=5.5$ cm and -5 cm $\leq z\leq 5$ cm. As plasma transport occurs mainly along magnetic field lines, the peak of n_{pl} measured by the LP at $r=3.5$ cm shows an increase of n_{pl} in the vicinity of the cathode. This means that a dc discharge sustained by the microwave plasma has probably developed. The increased plasma density near the cathode

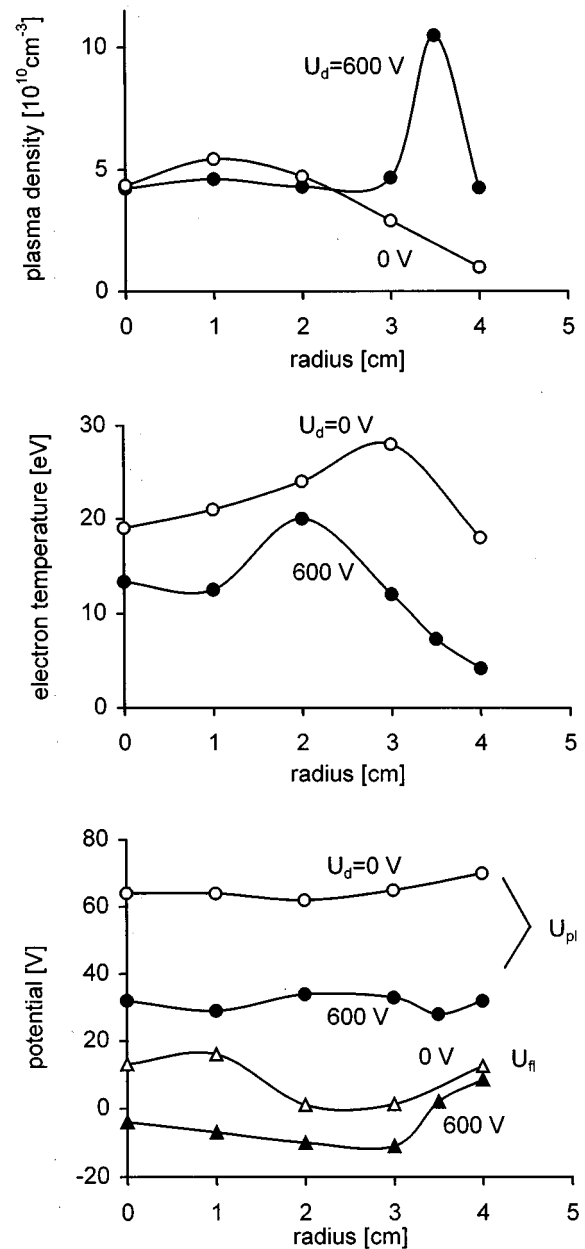


FIG. 10. Plasma density, electron temperature, plasma and floating potentials as a function of radius for $z=12$ cm, $p=5\times 10^{-3}$ Pa, $P_\mu=400$ W, two values of the cathode voltage $U_d=0$ V (open symbols) and $U_d=600$ V (solid symbols), $z_{\text{ECR}}=10$ cm and $MR=2.9$.

can be then ascribed to the action of secondary electrons from the cathode. Note that the dc power dissipated at the cathode $P_{dc}=600$ W is larger than the microwave power $P_\mu=400$ W.

The radial distributions of n_{pl} and T_e for $U_d=0$ V with the maxima off the axis reflect the radial distributions of the ionization rate and electron heating due to the absorption of microwaves. The distribution of microwave power density with a minimum at the axis is a consequence of the dependence of the refractive index of microwaves on the plasma density and, possibly, the occurrence of the plasma resonance absorption of the microwaves.²³ The plasma density is

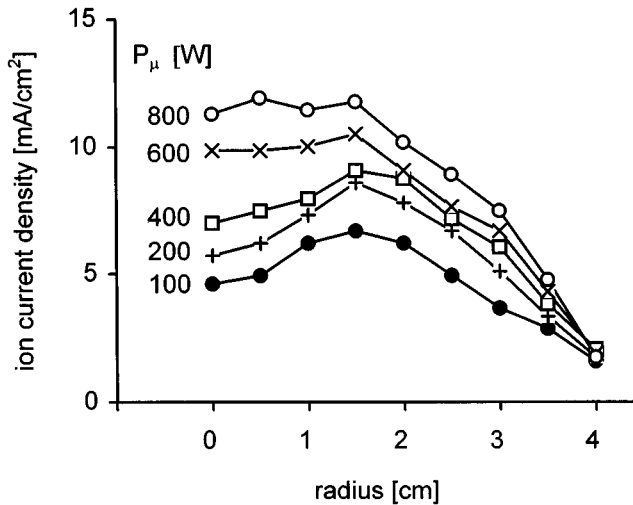


FIG. 11. The radial distribution of the saturated ion current density at $z_s=12$ cm for $p=5 \times 10^{-3}$ Pa, $U_d=0$ V, $z_{\text{ECR}}=10$ cm, $MR=2.9$ and P_μ ranging from 100 W to 800 W.

just about the value of the critical plasma density $n_{cr}=7 \times 10^{10}$ cm $^{-3}$ for the microwave frequency 2.45 GHz.

The radial distribution of the ion current density i_{sat}^+ also has a minimum at the axis. The minimum fills up with increasing microwave power; see Fig. 11. The values of the substrate ion current densities $i_{sat}^+ \approx 10$ mA/cm 2 may enable extensive ion assistance during the deposition of thin films.

The plasma parameters were also measured as a function of the microwave power and the cathode voltage; see Figs. 4 and 5. The increasing P_μ results in increasing T_e , U_{pl} and U_{fl} . Increasing U_d results mainly in decreasing U_{pl} . The consequences of these variations of plasma parameters for the confinement of the electrons were discussed above.

Heating and generation of the plasma by second harmonic resonance defined by $\omega=2\omega_{ce}$ (i.e., at $B=B_{\text{ECR}}/2=438$ G for $\omega=2\pi \times 2.45$ GHz) were reported in the literature, see Ref. 24, and references therein. Here, ω and ω_{ce} denote the driving and electron cyclotron angular frequencies, respectively, and B_{ECR} is the resonance magnetic field. In our experimental conditions, the second harmonic resonance itself was not able to ensure a stable generation of the discharge. This is confirmed by the fact that the discharge extinguished with the peak magnetic field B_{max} decreasing to below 900 G. In Ref. 22, it was suggested that the observed off-axis heating of the plasma electrons occurred at the second harmonic resonance zone which was located at the periphery of the plasma column (i.e., it did not intersect the device axis). However, this cannot explain the radial distribution of the electron temperature with an off-axis peak in Fig. 10, because in this case the second harmonic resonance zone fills the whole cross section of the cylindrical discharge chamber (the magnetic field at the bottom of the trap is $B_{min}=390$ G).²¹

IV. CONCLUSIONS

The measurements reported in this article show that ECR sputtering with the magnetic-mirror plasma confinement and

cylindrical hollow cathode is characterized by low working pressures 5×10^{-3} Pa $\leq p \leq 2 \times 10^{-2}$ Pa, cathode currents up to 1 A and high ion fluxes to the substrate up to 12 mA/cm 2 . These characteristics predestine this process for ion-assisted deposition of metal and compound thin films with controlled crystal structure.

Details of the operation of the sputtering apparatus were investigated. It was found that the cathode current is maximum when the ECR zone is less than about 10 cm from the center of the cathode. The electron confinement worsens with increasing microwave power and negative cathode bias due to increasing electron temperature and decreasing plasma potential, respectively. In this way the discharge is not self-sustained for large microwave powers and negative cathode biases if the electron confinement along the magnetic field lines is not sufficient. The electron confinement is improved by a larger MR and/or by a negatively biased substrate holder. The discharge was self-sustained at least up to $P_\mu=1.3$ kW and $U_d=1$ kV for $MR=2.9$ and substrate holder potential $U_s \leq U_{fl}$.

Measurements of the axial and radial distributions of the plasma parameters by Langmuir probe show that the plasma densities $n_{pl} \approx 10^{11}$ cm $^{-3}$ and electron temperatures $T_e \approx 25$ eV are maximum between the ECR zones and off the axis. The measurements revealed a decrease in electron temperature and a doubling of plasma density at positions connected to the cathode by magnetic field lines.

In a subsequent experiment ECR sputtering with magnetic-mirror confinement was used for deposition of crystalline TiNi thin films at low substrate temperatures $T_s \approx 300$ °C.²⁵

ACKNOWLEDGMENTS

One of the authors (M.M.) is grateful to the Japanese Ministry of Education, Science, Sports and Culture for the financial support during his stay at the Joining and Welding Research Institute, Osaka University, Japan.

¹T. Ono, C. Takahashi, and S. Matsuo, Jpn. J. Appl. Phys. **23**, L534 (1984).

²S. Takehiro, N. Yamanaka, H. Shindo, S. Shingubara, and Y. Horiike, Jpn. J. Appl. Phys. **30**, 3657 (1991).

³M. Mišina and J. Musil, Surf. Coat. Technol. **74-75**, 450 (1995).

⁴P. Kidd, J. Vac. Sci. Technol. A **9**, 466 (1991).

⁵Y. Yoshida, Rev. Sci. Instrum. **62**, 1498 (1991).

⁶M. Matsuoka and K. Ono, J. Appl. Phys. **65**, 4403 (1989).

⁷C. Takahashi, M. Kiuchi, T. Ono, and S. Matsuo, J. Vac. Sci. Technol. A **6**, 2348 (1988).

⁸M. Kadota, T. Kasanammi, and M. Minakata, Jpn. J. Appl. Phys. **31**, 3013 (1992).

⁹M. Matsuoka, K. Hoshino, and K. Ono, Proceedings of the International Symposium on 3d Transition-Semi-Metal Thin Films, Sendai, Japan, 1991, p. 29.

¹⁰S. Itabashi and H. Yoshihara, Thin Solid Films **221**, 79 (1992).

¹¹T. Goto, H. Masumoto, and T. Hirai, Jpn. J. Appl. Phys. **28**, L88 (1989).

¹²H. Masumoto, T. Goto, and T. Hirai, Appl. Phys. Lett. **55**, 498 (1989).

¹³T. Inukai, M. Matsuoka, and K. Ono, Thin Solid Films **257**, 22 (1995).

¹⁴M. Matsuoka and S. Tohno, J. Vac. Sci. Technol. A **13**, 2427 (1995).

- ¹⁵J. N. Kidder and W. J. Varhue, *J. Vac. Sci. Technol. A* **10**, 1414 (1992).
- ¹⁶M. Tuda, K. Ono, M. Taki, and K. Namba, *Jpn. J. Appl. Phys.* **33**, 1530 (1994).
- ¹⁷Y. Sakamoto and H. Kokai, *Jpn. J. Appl. Phys.* **32**, 3985 (1993).
- ¹⁸K. L. Junck and W. D. Getty, *J. Vac. Sci. Technol. A* **12**, 2767 (1994).
- ¹⁹M. D. Kilgore, H. M. Wu, and D. B. Graves, *J. Vac. Sci. Technol. B* **12**, 494 (1994).
- ²⁰J. Musil, M. Mišina, and M. Čepera, *Czech. J. Phys.* **46**, 353 (1996).
- ²¹M. Mišina, Y. Setsuhara, and S. Miyake, *Trans. JWRI* **24**, 11 (1995).
- ²²Y. Arata, S. Miyake, and H. Kishimoto, *Jpn. J. Appl. Phys.* **26**, 2079 (1987).
- ²³J. Musil, *Vacuum* **36**, 161 (1986).
- ²⁴O. A. Popov, in *Physics of Thin Films, Vol. 18: Plasma Sources for Thin Film Deposition and Etching*, edited by M. H. Francombe and J. L. Vossen (Academic, New York, 1994), pp. 142–144.
- ²⁵M. Mišina, Y. Setsuhara, and S. Miyake, *Jpn. J. Appl. Phys.* (in press).